

# Effect of an external magnetic field on the nematic-isotropic phase transition in mesogenic systems of uniaxial and biaxial molecules

Nababrata Ghoshal, Kisor Mukhopadhyay<sup>1</sup> and Soumen Kumar Roy<sup>2, \*</sup>

Department of Physics, Mahishadal Raj College,  
Mahishadal, Purba-Medinipur, West Bengal, India

<sup>1</sup>Department of Physics, Sundarban Mahavidyalaya,  
Kakdwip, South 24 Parganas, West Bengal, India

<sup>2</sup>Department of Physics, Jadavpur University,  
Kolkata - 700 032, India

## Abstract

Influence of an external magnetic field on the nematic-isotropic ( $N - I$ ) phase transition in a dispersion model of nematic liquid crystals, where the molecules are either perfectly uniaxial or biaxial (board-like), has been studied by Monte Carlo simulation. Using multiple histogram reweighting technique and finite size scaling analysis the order of the phase transition, the transition temperature at the thermodynamic limit and the stability limit of the isotropic phase below the transition temperature for different magnetic field strengths have been determined. The magnetic field dependence of the shift in  $N - I$  transition temperature is observed to be more rapid than that predicted by the standard Landau-de Gennes and Maier-Saupe mean field theories. We have shown that for a given field strength the shift in the transition temperature

---

\*Corresponding author. E-mail: skroy@phys.jdvu.ac.in, Tel: +91 9874741525; fax: +91 33 24146584

is higher for the biaxial molecules in comparison with the uniaxial case. The study shows that the  $N - I$  transition for the biaxial molecules is weaker than the well known weak first order  $N - I$  transition for the uniaxial molecules and the presence of the external magnetic field (up to a certain critical value) makes the transition much more weaker for both the systems. The estimate of the critical magnetic field ( $\sim 110 T$ ) for the common nematics is found to be smaller than the earlier estimates.

## 1 INTRODUCTION

The study of the behaviour of liquid crystals in presence of an external field (either electric or magnetic) has long been an active area of research because of its fundamental and technological importance. There have been several theoretical [1, 2, 4, 3, 5, 6, 7] and experimental [8, 9, 10, 11, 12, 13] reports dealing with different phase transition phenomena in presence of external electric and magnetic fields.

In absence of any external field nematic liquid crystals composed of anisotropic molecules, usually modeled as rod-like in shape, possess long-range orientational order due to sufficiently strong intermolecular forces and in the uniaxial nematic phase ( $N$ ) the molecules become aligned, on the average, along a single macroscopic direction called the director ( $\mathbf{n}$ ). The degree of this orientational order is characterized by the second rank tensor nematic order parameter  $Q$  [14]. With increasing temperature the order parameter of a thermotropic liquid crystal in the nematic phase decreases and jumps to zero as the liquid crystal undergoes a weakly first-order nematic-isotropic ( $N - I$ ) transition at a temperature  $T_{NI}$ . The orientational order no longer exists in the isotropic phase ( $I$ ). If an external field is applied, the director in the  $N$  phase, tends to align parallel to the direction of the field provided the liquid crystal material has a positive dielectric or diamagnetic anisotropy and becomes pinned at relatively weak fields although the orientational order increases only by a small amount. The transition temperature  $T_{NI}$  also gets shifted towards a higher value. In the presence of an external field a weak orientational order is induced even in the isotropic phase resulting in an anisotropic phase known as the *paranematic* phase ( $pN$ ). From theoretical studies [2, 4] it has been observed that when the external field is weak the  $N - I$  (or  $pN$ ) phase transition occurs with a finite jump in the nematic order parameter and the transition is first order in nature. As the field strength is increased the difference between the  $N$  phase

and the  $pN$  phase decreases and finally it vanishes at a classical critical point defined by a critical temperature ( $T_C$ ) and a critical field ( $B_C$ ). This critical end point is analogous to the classical critical points observed in liquid-vapour and ferromagnetic systems [15]. Above the critical point the  $I$  (or  $pN$ ) and the  $N$  phases become indistinguishable, the symmetries of the phases being the same. The effect of an external magnetic field on the  $N - I$  transition is analogous to the effect observed by the application of pressure at the liquid-gas transition, the paranematic phase being the analog of the liquid-gas coexistence phase.

There are several reports [8, 10, 11, 16] of experimentally observed electric field induced first-order isotropic-nematic phase transition since its earliest theoretical prediction based on the mean field theories of Maier-Saupe and Landau de-Gennes [14]. On the other hand similar studies in the presence of a magnetic field are relatively fewer. The influence of a magnetic field on the  $N - I$  transition was first studied by Rosenblatt [12]. His experimental observation demonstrated that the presence of a magnetic field of strength  $14.8 T$  shifts the  $N - I$  transition temperature only by a few milliKelvin. The reason behind this small change is the very low value of the anisotropy of diamagnetic susceptibility for the traditional liquid crystal materials [14]. In order to substantially alter the  $N - I$  transition temperature for the conventional calamitic liquid crystals the necessary magnetic field strength should be larger than  $100 T$  and the estimated critical value of the magnetic field is much higher than this [12, 17].

The experimental observation of a magnetic field induced first-order isotropic-nematic transition in a thermotropic liquid crystal has been reported only recently by Ostapenko et al [13] who also observed a much higher shift in the  $N - I$  transition temperature ( $\sim 0.8^\circ C$  at  $B = 23 T$ ). Observation of such pronounced effects became possible by the use of a new class (non-traditional) of liquid crystal molecules having a bent core and by using a high-field resistive magnet. However, Ostapenko et. al. could not reach the critical point of the system in their investigation where a magnetic field up to  $31 T$  was used.

The bent-core compounds have exhibited different fascinating phenomena in liquid crystal science, for example, the formation of the long searched biaxial nematic phase in thermotropic liquid crystals [18, 19] and the formation of chiral phases resulting from achiral molecules [20]. Another experimental study [21] has shown that the  $N - I$  transition in the bent-core compounds is more weakly first order as the value of  $T_{NI} - T_- \approx 0.4^\circ C$  which

is significantly below the values  $\sim 1^\circ C$  in typical calamitics,  $T_-$  being the super cooling limit of the isotropic phase. The exceptional behaviour of this new class of liquid crystals has been explained [21] by considering the isotropic phase to be composed of microscopic complexes or "clusters" of bent core molecules. Another important aspect of the bent-core mesogenic molecules is their inherent biaxiality. A mean-field study [7] was reported more than two decades ago in which the effect of an external magnetic field on biaxial nematogenic molecules was examined. It is evident from this work that as the degree of biaxiality is increased the critical field strength drops rapidly and for a given field strength the shift in  $T_{NI}$  is higher in uniaxial nematics composed of biaxial molecules. So far as our knowledge is concerned no other theoretical or computer simulation study on systems composed of biaxial molecules coupled with external magnetic field has been reported.

In this paper we have tried to investigate using Monte Carlo (MC) simulation the effect of an external magnetic field on the  $N - I$  (or  $N - pN$ ) transition. Using a lattice model of nematics where the particles interact via a dispersion potential we have performed the multiple histogram reweighting [22] and finite-size scaling analysis [23, 24] of our data. We have studied the magnetic field dependence of the transition temperature  $T_{NI}$  for systems composed of either uniaxial or biaxial molecules and have compared our results with that predicted by the mean field theory. We have also confirmed the first orderedness of the  $N - pN$  phase transition and find that the transition gets weaker with the increase in the magnetic field and ultimately reaches a critical point. Using the technique similar to that applied by Saito et. al. in a recent work [25] for the study of quark mass dependence of the finite temperature QCD phase transition, we have estimated the value of the critical magnetic field for the system composed of uniaxial molecules. The use of finite size scaling along with the multiple histogram reweighting has also enabled us to obtain the magnetic field dependence of the supercooling limit of the isotropic phase (or  $pN$  phase) in the thermodynamic limit. Expectedly we find that the difference  $T_{NI}(B) - T_-(B)$  decreases with the increase in the magnetic field and vanishes at a certain point  $(B_C, T_C)$  which we have identified as the critical point. Our work is intended to supplement the predictions of the mean field theory in this area where no other theoretical work has been reported. The MC simulations which have so far been performed to study the effects of external fields on the  $N - I$  transitions are the works of Luckhurst and coworkers [26] and that of Berardi et.

al. [27]. However these simulations do not address the features of the phase transitions we have described.

In the next section we describe the model employed in our simulation. This is followed by the computational details, results and conclusions.

## 2 THE DISPERSION POTENTIAL AND THE EFFECT OF THE MAGNETIC FIELD

We consider a system of biaxial prolate molecules possessing  $D_{2h}$  symmetry (board-like), whose centres of mass are associated with a simple-cubic lattice and subjected to an external magnetic field. The total energy of the system is the sum of two terms: (i) a dispersion potential term which takes into account the interaction between all nearest neighbour pairs of molecules and (ii) a field term which represents the interaction of each molecule with the external field. The dispersion term in the Hamiltonian contains a factor  $\lambda$  which is a measure of the molecular biaxiality. The case of uniaxial molecules ( $D_{\infty h}$  symmetry) is obtained by simply setting this parameter equal to zero.

The orientationally anisotropic dispersion pair interaction obtained from London dispersion model [28, 29] explicitly depends on both the mutual orientation of the two interacting molecules (say the  $i^{th}$  and  $j^{th}$  molecules), and on their orientations with respect to the intermolecular unit vector ( $\mathbf{r}_{ij}$ ). By isotropically averaging over the intermolecular unit vector,  $\mathbf{r}_{ij}$  the dispersion potential between two identical neighbouring molecules becomes [30, 31]

$$U_{ij}^{disp} = -\epsilon_{ij} \{R_{00}^2(\Omega_{ij}) + 2\lambda[R_{02}^2(\Omega_{ij}) + R_{20}^2(\Omega_{ij})] + 4\lambda^2 R_{22}^2(\Omega_{ij})\}. \quad (1)$$

Here  $\Omega_{ij} = \{\phi_{ij}, \theta_{ij}, \psi_{ij}\}$  denotes the triplet of Euler angles defining the relative orientation of  $i^{th}$  and  $j^{th}$  molecules; we have used the convention used by Rose [32] in defining the Euler angles.  $\epsilon_{ij}$  is the strength parameter which is assumed to be a positive constant ( $\epsilon$ ) when the particles  $i$  and  $j$  are nearest neighbours and zero otherwise.  $R_{mn}^L$  are combinations of symmetry-adapted ( $D_{2h}$ ) Wigner functions

$$R_{00}^2 = \frac{3}{2} \cos^2 \theta - \frac{1}{2} \quad (2)$$

$$R_{02}^2 = \frac{\sqrt{6}}{4} \sin^2 \theta \cos 2\psi \quad (3)$$

$$R_{20}^2 = \frac{\sqrt{6}}{4} \sin^2 \theta \cos 2\phi \quad (4)$$

$$R_{22}^2 = \frac{1}{4}(1 + \cos^2 \theta) \cos 2\phi \cos 2\psi - \frac{1}{2} \cos \theta \sin 2\phi \sin 2\psi. \quad (5)$$

The parameter  $\lambda$  is a measure of the molecular biaxiality and it depends on the molecular properties. For the dispersion interactions,  $\lambda$  can be expressed in terms of the eigenvalues  $(\rho_1, \rho_2, \rho_3)$  of the polarizability tensor  $\boldsymbol{\rho}$  of the biaxial molecule

$$\lambda = \sqrt{\frac{3}{2} \frac{\rho_2 - \rho_1}{2\rho_3 - \rho_2 - \rho_1}}. \quad (6)$$

The condition for the maximum biaxiality is  $\rho_3 - \rho_2 = \rho_2 - \rho_1 > 0$ ,  $\lambda = \lambda_C = 1/\sqrt{6}$  and this self-dual geometry corresponds to the Landau point in the phase diagram where a direct biaxial nematic to isotropic phase transition occurs.  $\lambda < \lambda_C$  corresponds to the case of prolate molecules whereas  $\lambda > \lambda_C$  corresponds to oblate molecules. This dispersion model can successfully reproduce both the uniaxial and the biaxial orientational orders and various order-disorder transitions as a function of temperature and molecular biaxiality. The phase diagram for this dispersion model has been well studied by mean field theory as well as Monte Carlo methods [30, 31]. In our simulations we consider two cases - in one case  $\lambda = 0$  and the pair potential takes the usual Lebwohl-Lasher (LL) form [33] for nematic liquid crystals of perfectly uniaxial molecules which has been extensively studied by Zhang et al [34]. In the other case we choose  $\lambda = 0.2$  which represents a biaxial system composed of prolate biaxial molecules. For the LL model (uniaxial one) there is a single weak first-order  $N-I$  transition at a dimensionless temperature  $T = 1.1232 \pm 0.0001$  [34, 35]. From the Monte Carlo results, as reported in [31, 36], the biaxial model ( $\lambda = 0.2$ ) exhibits a biaxial-uniaxial phase transition at low temperature ( $T \approx 0.2$ ) and a uniaxial-isotropic transition at higher temperature ( $T \approx 1.1$ ). The biaxial nematic-uniaxial nematic transition is known to be second order while the uniaxial nematic-isotropic transition is first order. The dimensionless temperature has been defined as  $T = k_B T_K / \epsilon$ ,  $T_K$  being the temperature measured in Kelvin.

The interaction of a uniform external magnetic field  $\mathbf{B}$  chosen along the laboratory  $Z$  axis (unit vector  $\mathbf{z}$ ), with the  $i$ th molecule resulting from its coupling with the longest molecular symmetry axis  $\mathbf{w}_i$  is taken as

$$U_i^{field} = -\epsilon \xi \left[ \frac{3}{2} (\mathbf{w}_i \cdot \mathbf{z})^2 - \frac{1}{2} \right]. \quad (7)$$

Where,  $\xi$  is a dimensionless quantity which determines the strength of coupling of the molecular symmetry axis with the magnetic field and is given by

$$\xi = \frac{(\Delta\kappa)B^2}{3\mu_0\epsilon}.$$

Here,  $\Delta\kappa = \kappa_{\parallel} - \kappa_{\perp}$  is the anisotropy of the molecular magnetic polarizability and  $\mu_0$  is the permeability of the free space. In the simulations we take  $\xi$  to be a positive quantity so that the molecules tend to get their long axes aligned along the magnetic field.

The total energy  $\mathcal{E}$  of the system is therefore given by

$$\mathcal{E} = \sum_{\langle i,j \rangle} U_{ij}^{disp} + \sum_i U_i^{field} \quad (8)$$

where, the  $\langle \rangle$  bracket represents the nearest neighbours and the two terms on the right hand side are obtained from Eqs. 1 and 7.

### 3 COMPUTATIONAL ASPECTS

To calculate the thermodynamic observables of interest as a function of  $\lambda$ ,  $\xi$  and  $T$  we have performed a series of Monte Carlo (MC) simulations using the conventional Metropolis algorithm on a periodically repeated simple cubic lattice, for four system sizes. A Monte Carlo move was attempted by selecting a site at random and then by choosing one of the laboratory axes at random and rotating the molecule at that site about the chosen laboratory axis following the Barker-Watts method [37]. For generating histograms of energy and the constant energy averages of the order parameter and its square, simulations were run in cascade, in order of increasing temperature  $T$  for a given set of values of  $\lambda$  and  $\xi$ .

We have used  $10^6$  sweeps or MCS (Monte Carlo steps per site) for the equilibration and  $(4-6) \times 10^6$  MCS for the production run for every set of values of  $\lambda$ ,  $\xi$  and  $T$ . For the largest lattice size ( $L = 30$ ), the total run length is more than 10 000 times the correlation time. We have divided the total run into several (100) blocks by performing independent simulations for each set of values of  $L$ ,  $\lambda$ ,  $\xi$  and  $T$  so that we could compute the jackknife errors [38]. In order to analyze the orientational order we have calculated the second rank order parameters  $\langle R_{mn}^2 \rangle$  following the procedure described by Vieillard-Baron [39]. According to this, a  $\mathbf{Q}$  tensor is defined for the molecular axes associated with a reference molecule. For

an arbitrary unit vector  $\mathbf{w}$ , the elements of the  $\mathbf{Q}$  tensor are defined as

$$Q_{\alpha\beta}(\mathbf{w}) = \langle (3w_\alpha w_\beta - \delta_{\alpha\beta})/2 \rangle \quad (9)$$

where the average is taken over the configurations and the subscripts  $\alpha$  and  $\beta$  label Cartesian components of  $\mathbf{w}$  with respect to an arbitrary laboratory frame. By diagonalizing the matrix one obtains nine eigenvalues and nine eigenvectors which are then recombined to give the four order parameters  $\langle R_{00}^2 \rangle$ ,  $\langle R_{02}^2 \rangle$ ,  $\langle R_{20}^2 \rangle$  and  $\langle R_{22}^2 \rangle$  with respect to the director frame [40].

Out of these four second rank order parameters the usual uniaxial order parameter  $\langle R_{00}^2 \rangle$  (or,  $S$ ) which measures the alignment of the longest molecular symmetry axis with the primary director ( $\mathbf{n}$ ), is involved in our study. The full set of order parameters are required to describe completely the biaxial nematic phase of a system of biaxial molecules. In our work we have simulated a very short temperature range in the higher sides of  $T$  within which no biaxial phase occurs.

We have calculated the reduced specific heat per particle and the ordering susceptibility from fluctuations in the energy and the order parameter respectively

$$C_v = \frac{\langle E^2 \rangle - \langle E \rangle^2}{Nk_B T^2} \quad (10)$$

$$\chi = \frac{N(\langle R_{00}^2 \rangle - \langle R_{00}^2 \rangle^2)}{T} \quad (11)$$

where  $E$  is the scaled total energy of the system.

Various thermodynamic quantities have been computed using the multiple-histogram reweighting method proposed by Ferrenberg and Swendsen [22]. In our simulations we have generated the energy histogram for certain values of the dimensionless temperature  $T$  and corresponding to each energy bin we have generated (constant energy) averages of the order parameter and its square. These averages are used to evaluate the order parameter and the corresponding susceptibility as a function of temperature using the reweighting method.



## 4 RESULTS AND DISCUSSION

### 4.1 Probability distribution functions and free energy for the uniaxial and the biaxial models

In order to analyse the effect of the external field on the phase behaviour of nematic liquid crystals we need to simulate the models within a very narrow range of temperature ( $T = 1.110$  to  $1.140$ ) around  $T_{NI}$ . We aimed at getting the transition temperatures with an accuracy of  $\pm 0.0001$  and have therefore used the multiple histogram reweighting technique for the purpose.

We have performed extensive Monte Carlo simulation for different values of the external field parameter  $\xi$  at five or six different temperatures within the said temperature range to generate histograms for both the uniaxial and the biaxial models for  $L = 18, 22, 26$  and  $30$ . For the uniaxial molecules simulations have been performed for five different values of  $\xi$  ranging from  $0$  to  $0.00125$  with an increment of  $0.000375$  for each lattice size, while for the biaxial model five different values of  $\xi$  from  $0$  to  $0.001$  with an increment of  $0.00025$  have been used. Thus a total of about  $200$  simulations were performed for different values of  $\lambda$ ,  $L$ ,  $\xi$  and  $T$ . The histograms were used to obtain the temperature dependence of internal energy  $\langle E \rangle$ , order parameter  $\langle R_{00}^2 \rangle$  and the corresponding response functions i.e. the specific heat ( $C_v$ ) and the order parameter susceptibility ( $\chi$ ).

The results for the normalized histogram count  $P(E) = h(E)/\sum_E h(E)$  in absence of an external magnetic field for both  $\lambda = 0$  and  $\lambda = 0.2$  have been plotted in Figs. 1 and 2 respectively for the  $L = 30$  lattice. These figures show an evidence of double peak like structures which are however not well separated and are more so in Fig 2. These merely confirm the well known weakly first order nature of the  $N - I$  transition which gets weaker for the biaxial molecules. With increase in the strength of the magnetic field the overlap in the double peak like structures are found to increase even more for both values of  $\lambda$ .

We have derived the relevant part of the free-energy like functions  $A(E)$  from the energy distribution functions,  $P(E)$  for both  $\lambda = 0$  and  $\lambda = 0.2$  using the relation  $A(E) = -\ln P(E)$ . For the uniaxial molecules we have shown (Fig. 3) the field dependence of the free energy  $A$  at finite size transition for the largest simulated system size (i.e. for  $L = 30$ ) for which the free energy barrier between the two minima is well pronounced and the effect of the

external field on  $\Delta F$  is clearly visible. Here, the bulk free energy,  $\Delta F$  is given by  $\Delta F(\xi, L) = A(E_m; T, \xi, L) - A(E_1; T, \xi, L)$  where  $E_1$  is the energy at which either of the two minima of  $A$  (of equal depth) appears and  $E_m$  gives the position of the maximum of the free energy  $A$ . The temperatures in all cases were adjusted to obtain two minima of equal depth. We observe that the double-well becomes shallower as  $\xi$  increases. The external field thus reduces the strength of the first order transition and this suggests that for a particular value of the field ( $\xi_c(L)$ ) the barrier between the two minima of  $A(E)$  is likely to vanish which would correspond to the end point where the first order phase transition turns into a crossover [25].

The mesogenic molecules having biaxiality  $\lambda = 0.2$  however does not show any noticeable energy barrier separating the two minima in  $A$ , even in absence of the external magnetic field and for the largest system size ( $L = 30$ ) simulated (Fig. 4). This observation thus does not provide any conclusive evidence about the nature of the nematic-isotropic transition for the system of biaxial molecules. This is true for the system sizes we have investigated and it is likely that using systems of significantly larger size one could observe the free energy barrier for  $\lambda = 0.2$  and its dependence on the magnetic field.

## 4.2 Finite size scaling and the shift in NI transition temperature with increasing magnetic field

For finite systems the peak height of  $C_v$  increases with increasing system size and the scaling relation for  $C_v^{max}$  in a first-order phase transition obeys  $C_v^{max} \sim L^d$  [23, 24]. We see that this scaling relation holds good for the uniaxial system (Fig. 5). The data fit well for all values of  $\xi$  used in our simulations. The expected linear fits of  $\chi^{max}$  are presented in Fig. 6 for the uniaxial molecules. We have observed that with increasing  $\xi$  the heights of the maxima  $C_v^{max}(L)$  and  $\chi^{max}(L)$  are suppressed particularly for the higher lattice sizes  $L = 26$  and  $30$ . This observation shows that the presence of magnetic field weakens the first orderedness of the  $N - I$  transition.

In case of biaxial system the straight line fits (Figs. 7 and 8) to the data of the peak heights of  $C_v$  and  $\chi$  for  $\xi = 0, 0.00025, 0.0005$  and  $0.00075$  show that the  $N - I$  transition obeys the first-order scaling laws for this system too. Determining the finite-size transition temperature ( $T_{NI}(L)$ ) from the location of the maximum of the specific heat and the su-

ceptibility curves we have used the scaling relation  $T_{NI}(L) - T_{NI} \sim L^{-d}$  and performing a linear extrapolation to the thermodynamic limit ( $L \rightarrow \infty$ ) the transition temperature  $T_{NI}$  in the thermodynamic limit was estimated. In Fig. 9 the linear fits of the data for  $T_{NI}(L)$  obtained from both  $C_v$  and  $\chi$  plots for the uniaxial molecules are shown and in Fig. 10 the same are plotted for the biaxial molecules. The estimated transition temperatures at the thermodynamic limit are listed in Table-1. We find the expected increase in  $T_{NI}$  with increase in  $\xi$  for both  $\lambda = 0$  and  $\lambda = 0.2$ . The shift  $\delta T_{NI}$  in the transition temperature is plotted against  $\xi$  ( $\xi \propto B^2$ ) in Fig. 11. We obtain good quadratic fits to the data in both cases. The quadratic variations of  $\delta T_{NI}$  with  $\xi$  do not follow the prediction of the Landau de Gennes model for the isotropic-nematic transition which predicts a linear variation of  $\delta T_{NI}$  with  $B^2$ . The quadratic functions used for the fits are  $f(\xi) = 5.7 \times 10^{-6} + 0.57\xi + 950.86\xi^2$  for  $\lambda = 0$  and  $g(\xi) = 8.5 \times 10^{-6} + 0.77\xi + 1028.57\xi^2$  for  $\lambda = 0.2$ . Therefore, the rise of  $T_{NI}$  over its zero-field value is steeper for the biaxial molecules than that for the uniaxial molecules. For low magnetic fields the slope of the fit for  $\lambda = 0.2$  is 35% higher than that for  $\lambda = 0$ . The results suggest that the external magnetic field necessary for inducing the  $I(pN) - N$  phase transition is lower for the biaxial system than the uniaxial system (where initial temperatures for both systems are assumed to be equally higher than their respective zero-field transition temperatures,  $T_{NI}(0)$ ). The mean field study of Wojtowicz and Sheng [4] for the uniaxial model shows that the slope of a linear fit is lower by 20% in comparison to the slope extracted from Fig.3 of Ref.[7] in which the model under investigation was biaxial. Our observation regarding the shift in  $T_{NI}$  with increase in magnetic field is therefore consistent with the mean field results.

The finite size stability limit,  $T_-(L)$  of the isotropic phase for uniaxial molecules is estimated as the temperature where the second, local minimum (at higher energy) of  $A$  just vanishes as  $T$  is gradually lowered below  $T_{NI}$ . From extrapolation to the thermodynamic limit we estimate  $T_-$  for different field strengths as indicated in Fig. 9 by dashed lines.

### 4.3 Estimate of the critical field

An important observation is that the width of the stability limit of the  $I$  phase,  $T_{NI}(B) - T_-(B)$  decreases with increase in magnetic field (Fig. 12). From the fit to the data (as shown in Fig. 12) we find that the temperature difference  $T_{NI}(B) - T_-(B)$  varies linearly

with the field parameter  $\xi$  (i.e., quadratic in  $B$ ). With increasing magnetic field the weak first order  $N - I$  transition of the uniaxial model becomes weaker and  $T_-(B)$  gradually becomes closer to  $T_{NI}(B)$  and at the critical end point they merge into a single point. It is, therefore, possible to obtain an estimate of the critical magnetic field by performing a linear extrapolation (Fig. 12) up to the field strength ( $\xi_C$ ) at which  $T_{NI}(B) - T_-(B)$  becomes zero. For the uniaxial case we get  $\xi_C = 0.00130$ . In order to get an estimate of  $\xi$  in real units we may express the magnetic field as  $B = (3\mu_0\epsilon\xi/\Delta\kappa)^{1/2}$ . The energy unit  $\epsilon$  can be estimated by using the experimental and simulated nematic-isotropic transition temperatures, i.e.  $\epsilon = k_B T_K(B = 0)/T_{NI}(B = 0)$ . For a common nematic, say MBBA, the  $N - I$  transition temperature  $T_K(B = 0) = 320K$  and the anisotropy of the molecular magnetic polarizability  $\Delta\kappa \approx 0.16 \times 10^{-32} m^3$  [41]. Using these values and the simulated value of  $T_{NI}(B = 0) = 1.1232$  for  $\lambda = 0$  we can obtain  $B \approx 3040\sqrt{\xi} T$ . Therefore, the critical magnetic field  $B_C$  for common nematics corresponding to our estimate,  $\xi_C = 0.00130$ , is  $\sim 110 T$ .

We can also obtain a finite size estimate of  $\xi_C(L)$  from the field dependence of  $\Delta F$  [25] as shown in Fig. 13. We observe that as the field strength parameter  $\xi$  is increased beyond 0.00125 the free energy barrier decreases much faster. For the uniaxial molecules we may estimate the value of  $\xi_c$  by performing a linear extrapolation using the results of the barrier height ( $\Delta F$ ) for three higher values of  $\xi$  i.e. 0.00125, 0.0013 and 0.0014 (we have extended our simulations to  $\xi = 0.0013$  and 0.0014 for the largest lattice size  $L = 30$ ). Our estimate of the finite size critical field parameter is  $\sim 0.00148$  which results in a value of the critical field  $B_C$  for the common nematogens to be  $\sim 120 T$ . This is larger than the estimate in thermodynamic limit given in the previous paragraph. Our estimate of the critical magnetic field is of the same order of magnitude (130  $T$ ) mentioned in [10] obtained from the phenomenological Landau-de Gennes theory and using the experimental values of the  $f$  parameters for 5CB. But the critical magnetic field predicted by the molecular theory of Maier-Saupe [4] is much higher (1000  $T$ ) than our estimate.

The corresponding critical temperature can be estimated from the extrapolation of the fitted curve for  $\lambda = 0$  in Fig.11 which gives  $T_C = 1.12555$ ,  $\delta T_C$  being 0.00235.

## 5 CONCLUSIONS

We have determined the shift in the  $N - I$  transition temperature with increasing external magnetic field in the thermodynamic limit for two nematic systems composed of uniaxial and biaxial molecules. These results represent the first numerical evidence of the first order nature of nematic-isotropic transition in an external magnetic field the presence of which makes the first order character weaker. The first order nature of the transition is established from the finite-size scaling behaviour of the transition temperature  $T_{NI}(L)$  obtained from the specific heat and susceptibility data.

The quadratic dependence of  $\delta T_{NI}$  with  $\xi$  where  $\xi \propto B^2$ , for both cases  $\lambda = 0$  and  $\lambda = 0.2$ , does not agree with the theoretical prediction of LDG model which predicts this to be linear for low values of the external magnetic field. The steeper nature of the quadratic fit for the biaxial molecules in comparison to that of the uniaxial molecules shows that a lower magnetic field strength is capable of inducing the isotropic-nematic transition for the biaxial case.

The free energy like quantity generated by the reweighting technique gives detailed insight of the equilibrium properties of the models in presence of an external magnetic field. In particular, for the uniaxial case, the effect of an external magnetic field on the free energy barrier is clearly observed. Our results show that the width of the stability limit of the isotropic phase below  $T_{NI}(B)$  decreases quadratically with the external field. We estimate the critical magnetic field strength for a system of uniaxial mesogenic molecules ( $\sim 110 T$ ). For the biaxial system we have not found any double well structure in the free energy. The work further suggests that the first order nature of the nematic-isotropic transition of a system of biaxial molecules is considerably weaker than that shown by the uniaxial LL model. The presence of an external magnetic field further weakens the first orderedness of the NI transition. To study the effect of magnetic field on the nematics composed of biaxial molecules systems of much bigger sizes need to be simulated.

## 6 ACKNOWLEDGMENT

NG acknowledges the award of a teacher fellowship under Faculty Development Programme of UGC, India, and KM is grateful to the UGC for the award of a minor research project.

## References

- [1] M. J. Freiser and R. J. Joenk, Phys. Letters **24A**, 683 (1967).
- [2] J. Hanus, Phys. Rev. **178**, 420 (1969).
- [3] C. P. Fan and M. J. Stephen, Phys. Rev. Lett. **25**, 500 (1970).
- [4] P. J. Wojtowicz and P. Sheng, Phys. Letters **48A**, 235 (1974).
- [5] J. Shen and C. W. Woo, Phys. Rev. A **24**, 493 (1981).
- [6] R. M. Hornreich, Phys. Letters **109A**, 232 (1985).
- [7] D. K. Remler and A. D. J. Haymet, J. Phys. Chem. **90**, 5426 (1986).
- [8] W. Helfrich, Phys. Rev. Lett. **24**, 201 (1970).
- [9] A. J. Nicastro and P. H. Keyes, Phys. Rev. A **30**, 3156 (1981).
- [10] I. Lelidis and G. Durand, Phys. Rev. E **48**, 3822 (1993).
- [11] I. Lelidis, M. Nobili and G. Durand, Phys. Rev. E **48**, 3818 (1993).
- [12] C. Rosenblatt, Phys. Rev. A **24**, 2236 (1981).
- [13] T. Ostapenko, D. B. Wiant, S. N. Sprunt, A. Jakli, and J. T. Gleeson, Phys. Rev. Lett. **101**, 247801 (2008).
- [14] P. G. de Gennes and J. Prost, *The Physics of Liquid Crystals*, (Oxford Science, Oxford, 1993).
- [15] H. E. Stanley, *Introduction to Phase Transition and Critical Phenomena*, (Oxford University Press, Oxford, 1971).
- [16] S. Dhara and N. V. Madhusudana, Eur. Phys. J. E **22**, 139 (2007).
- [17] J. Shen and C. Woo, Phys. Rev. A **24**, 493 (1981).
- [18] L. A. Madsen, T. J. Dingemans, M. Nakata, and E. T. Samulski, Phys. Rev. Lett. **92**, 145505 (2004).

- [19] B. R. Acharya, A. Primak, and S. Kumar, Phys. Rev. Lett. **92**, 145506 (2004).
- [20] D. R. Link, G. Natale, R. Shao, J. E. MacLennan, N. A. Clark, E. Korblova, and D. M. Walba, Science **278**, 1924 (1997).
- [21] D. Wiant, S. Stojadinovic, S. Sharma, K. Fodor-Csorba, A. Jakli, J. T. Gleeson, and S. Sprunt, Phys. Rev. E **73**, 030703(R) (2006).
- [22] A. M. Ferrenberg and R. H. Swendsen, Phys. Rev. Lett. **61**, 2635 (1988); **63**, 1195 (1989).
- [23] J. Lee and J. M. Kosterlitz, Phys. Rev. Lett. **65**, 137 (1990).
- [24] J. Lee and J. M. Kosterlitz, Phys. Rev. B **43**, 3265 (1991).
- [25] H. Saito, S. Ejiri, S. Aoki, T. Hatsuda, K. Kanaya, Y. Maezawa, H. Ohno, and T. Umeda, Phys. Rev. D **84**, 054502 (2011).
- [26] G. R. Luckhurst, P. Simpson and C. Zannoni, Chem. Phys. Lett. **78**, 429 (1981); G. R. Luckhurst and G. Saielli, J. Chem. Phys., **112**, 4342 (2000).
- [27] R. Berardi, S. Orlandi and C. Zannoni, Mol. Cryst. Liq. Cryst., P. L. Nordio Memorial issue, 2002.
- [28] A. D. Buckingham, in *Intermolecular Forces*, edited by J. O. Hirschfelder (Wiley, London, 1967), Chap. 2 [Adv. Chem. Phys. **12**, 107 (1967)].
- [29] A. J. Stone, *The Theory of Intermolecular Forces*, (Oxford University Press, Oxford, UK, 1997).
- [30] G. R. Luckhurst and S. Romano, Mol. Phys. **40**, 129 (1980).
- [31] F. Biscarini, C. Chiccoli, P. Pasini, F. Semeria, and C. Zannoni, Phys. Rev. Lett. **75**, 1803 (1995).
- [32] M. E. Rose, *Elementary Theory of Angular Momentum*, (Wiley, New York, 1957).
- [33] P. A. Lebowitz and G. Lasher, Phys. Rev. A **6**, 426 (1972).
- [34] Z. Zhang, O. G. Mouritsen, and M. J. Zuckermann, Phys. Rev. Lett. **69**, 2803 (1992).

- [35] U. Fabbri and C. Zannoni, *Mol. Phys.* **58**, 763 (1986).
- [36] N. Ghoshal, K. Mukhopadhyay and S. K. Roy, *Liq. Cryst.* **39**, 1381 (2012); arXiv:1205.6639v1 [cond-mat.soft] (2012).
- [37] J. A. Barker and R. O. Watts, *Chem. Phys. Lett.* **3**, 144 (1969).
- [38] M. E. J. Newman and G. T. Barkema, *Monte Carlo Methods in Statistical Physics*, (Clarendon press, Oxford, 1999).
- [39] J. Vieillard-Baron, *J. Chem. Phys.* **56**, 4729 (1972).
- [40] P. J. Camp and M. P. Allen, *J. Chem. Phys.* **106**, 6681 (1997).
- [41] W. H. de Jeu, *Physical properties of liquid crystalline materials*, Gordon and Breach Science Publishers, London, 1979.

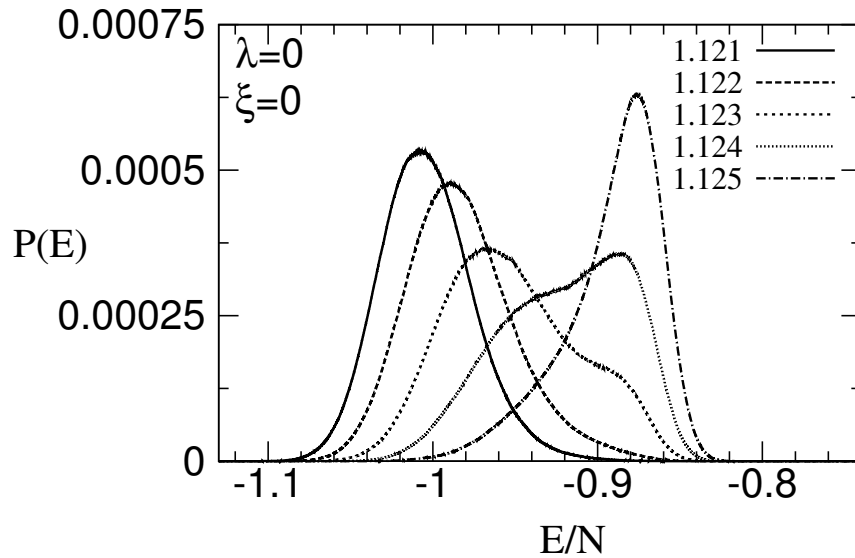


Figure 1: Normalized histogram for five different temperatures  $T = 1.121, 1.122, 1.123, 1.124$  and  $1.125$  for the uniaxial model ( $\lambda = 0$  and  $L = 30$ ) in absence of an external magnetic field.



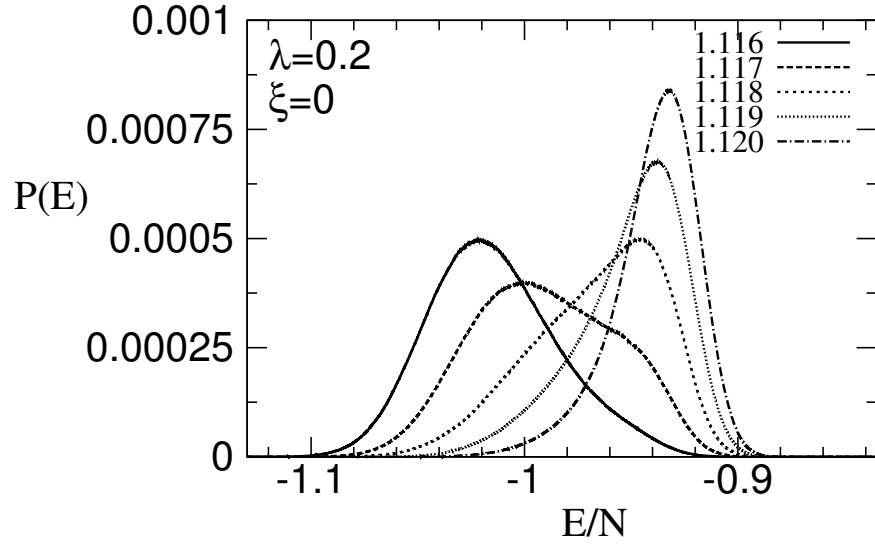


Figure 2: Normalized histogram for five temperatures for the biaxial model ( $\lambda = 0.2$  and  $L = 30$ ) in absence of an external magnetic field.

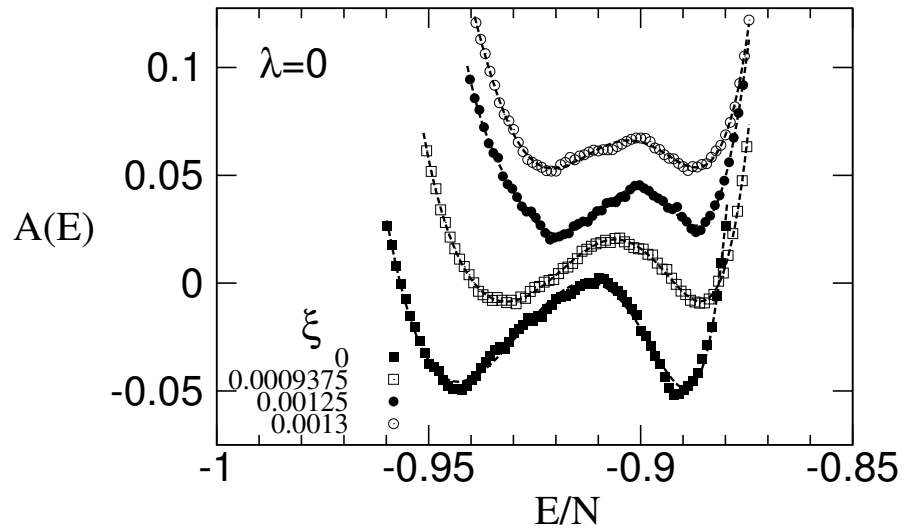


Figure 3: Free energy  $A$  as a function of energy per molecule with and without external magnetic field for the uniaxial model for  $L = 30$ . From bottom to top the field parameters are 0 (■), 0.0009375 (□), 0.00125 (●) and 0.0013 (○). An eighth-order polynomial fit to the data is also presented.

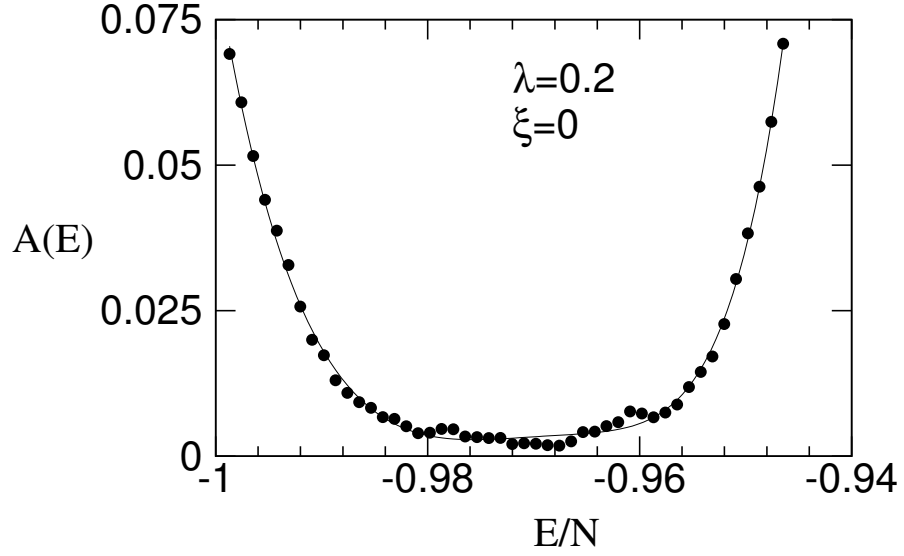


Figure 4: Free energy  $A$  as a function of energy per molecule without any external field for the biaxial model for  $L = 30$ .

Table 1: NI transition temperatures (at thermodynamic limit) for different values of the external field strength parameter  $\xi$  for the uniaxial and the biaxial systems. Estimates of the super cooling limits  $T_-$  are also listed for the uniaxial system. The estimated (jackknife) error in each temperature is  $\pm 0.0001$ .

| $\lambda$ | $\xi$     | $T_{NI}$ (from $C_V vs T$ ) | $T_{NI}$ (from $\chi vs T$ ) | $T_-$  |
|-----------|-----------|-----------------------------|------------------------------|--------|
|           | 0         | 1.1232                      | 1.1232                       | 1.1221 |
|           | 0.0003125 | 1.1234                      | 1.1234                       | 1.1226 |
| 0         | 0.0006250 | 1.1238                      | 1.1239                       | 1.1233 |
|           | 0.0009375 | 1.1245                      | 1.1245                       | 1.1242 |
|           | 0.0012500 | 1.1254                      | 1.1255                       |        |
|           | 0         | 1.1166                      | 1.1167                       |        |
|           | 0.00025   | 1.1169                      | 1.1170                       |        |
| 0.2       | 0.00050   | 1.1172                      | 1.1173                       |        |
|           | 0.00075   | 1.1178                      | 1.1179                       |        |
|           | 0.00100   | 1.1184                      | 1.1185                       |        |

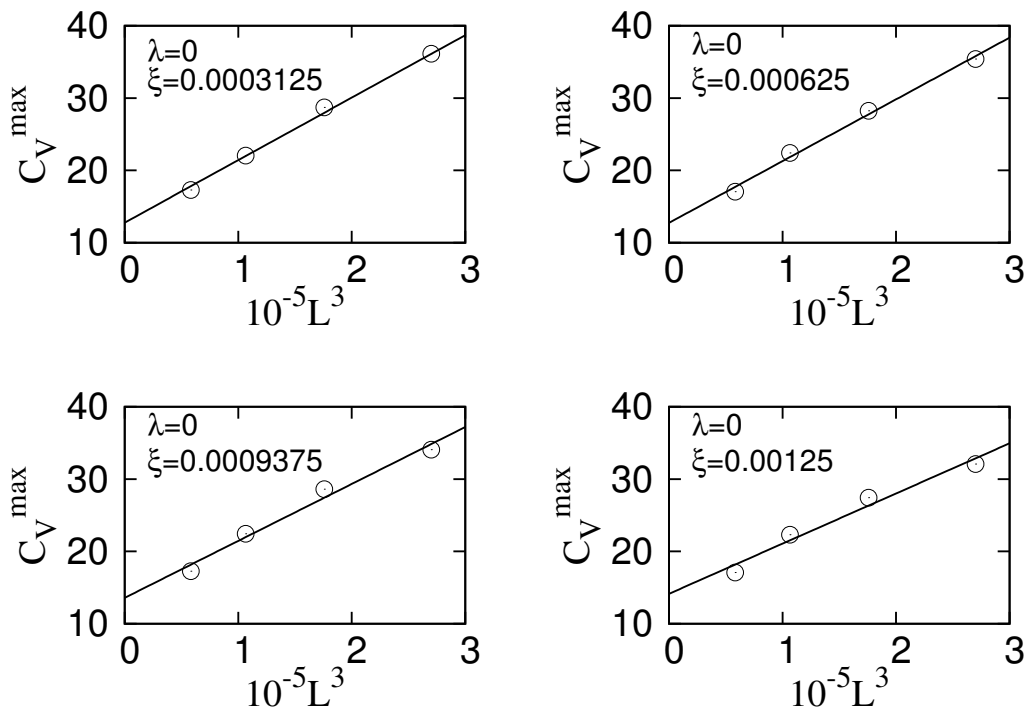


Figure 5: Finite-size scaling behaviours of the peak height of  $C_v$  for the uniaxial molecules for four different values of the field strength parameter  $\xi = 0.0003125 - 0.00125$ . The estimated errors are of the order of the size of the symbols.

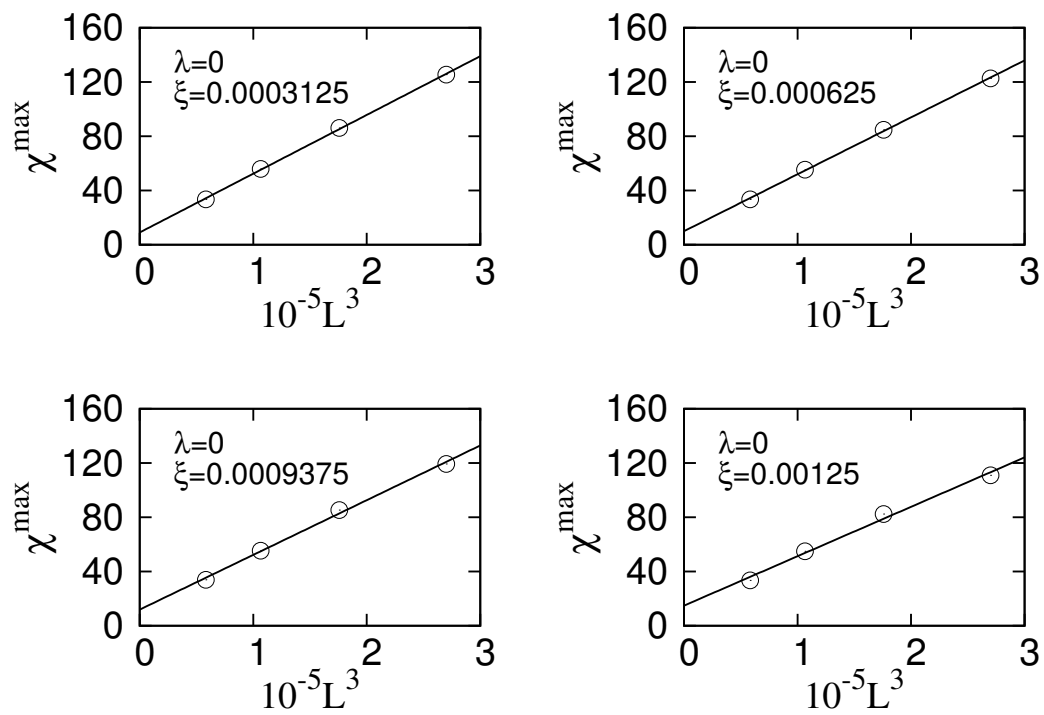


Figure 6: Finite-size scaling behaviours of the peak height of  $\chi$  for the uniaxial molecules for four different values of the field strength parameter  $\xi = 0.0003125 - 0.00125$ . The estimated errors are of the order of the size of the symbols.

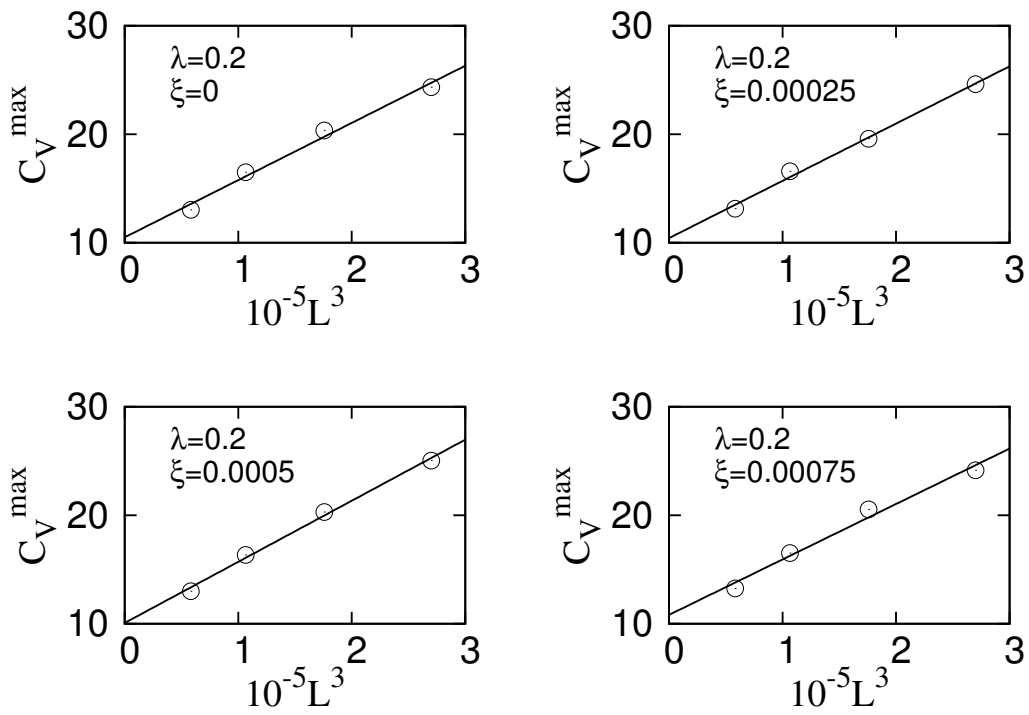


Figure 7: Finite-size scaling behaviours of the peak height of  $C_v$  for the biaxial molecules for four different values of the field strength parameter  $\xi = 0 - 0.00075$ . The estimated errors are of the order of the size of the symbols.

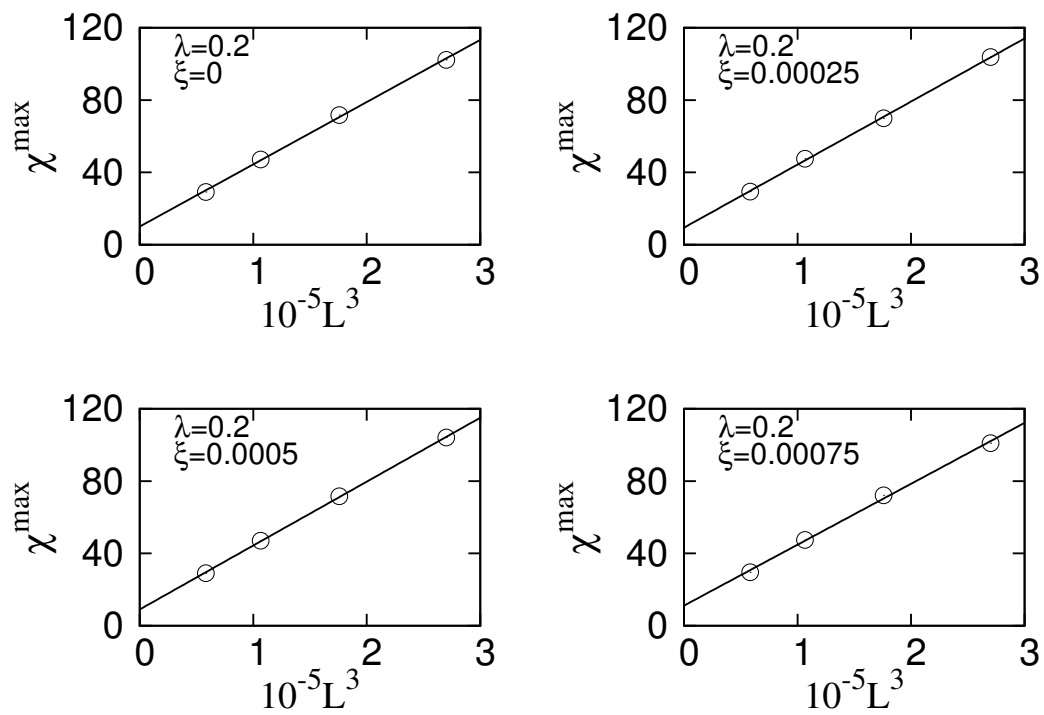


Figure 8: Finite-size scaling behaviours of the peak height of  $\chi$  for the biaxial molecules for four different values of the field strength parameter  $\xi = 0 - 0.00075$ . The estimated errors are of the order of the size of the symbols.

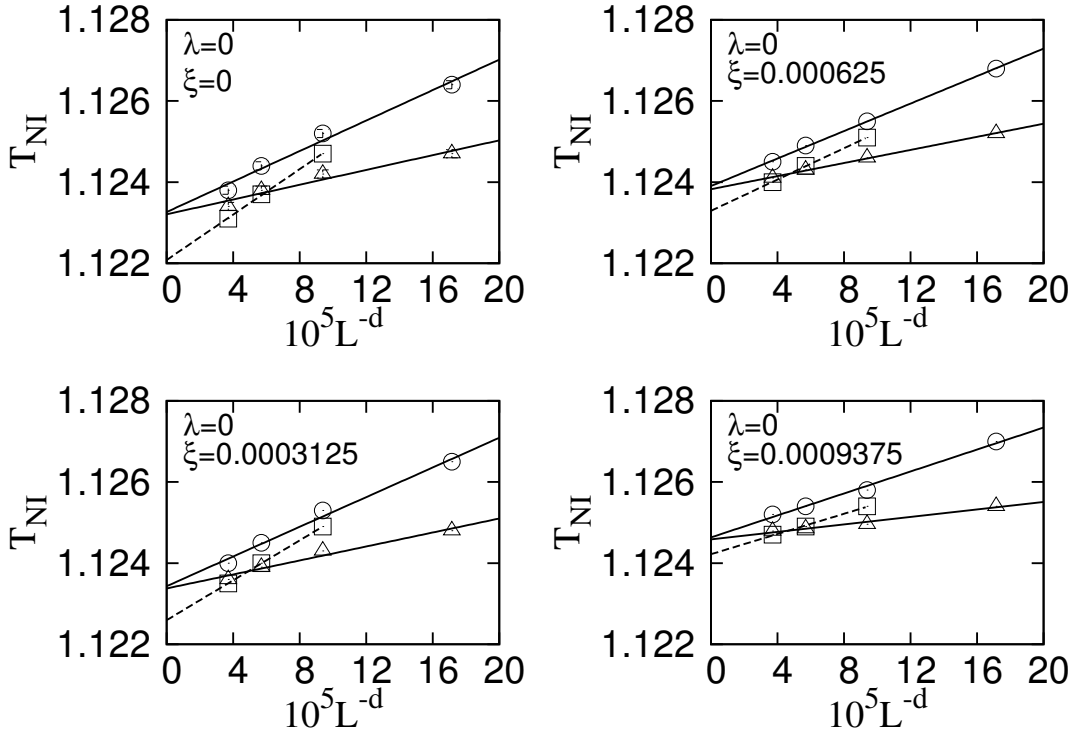


Figure 9: Finite-size scaling behaviour shown for two different measures of  $T_{NI}(L)$  for the uniaxial system at four different values of  $\xi$  (the data points represented by  $\Delta$  and  $\circ$  are obtained from the peaks of  $C_v$  and  $\chi$  respectively). The estimates of  $T_-(L)$  are also shown ( $\square$ ). Extrapolations to the thermodynamic limits are denoted by solid and dashed lines, respectively.

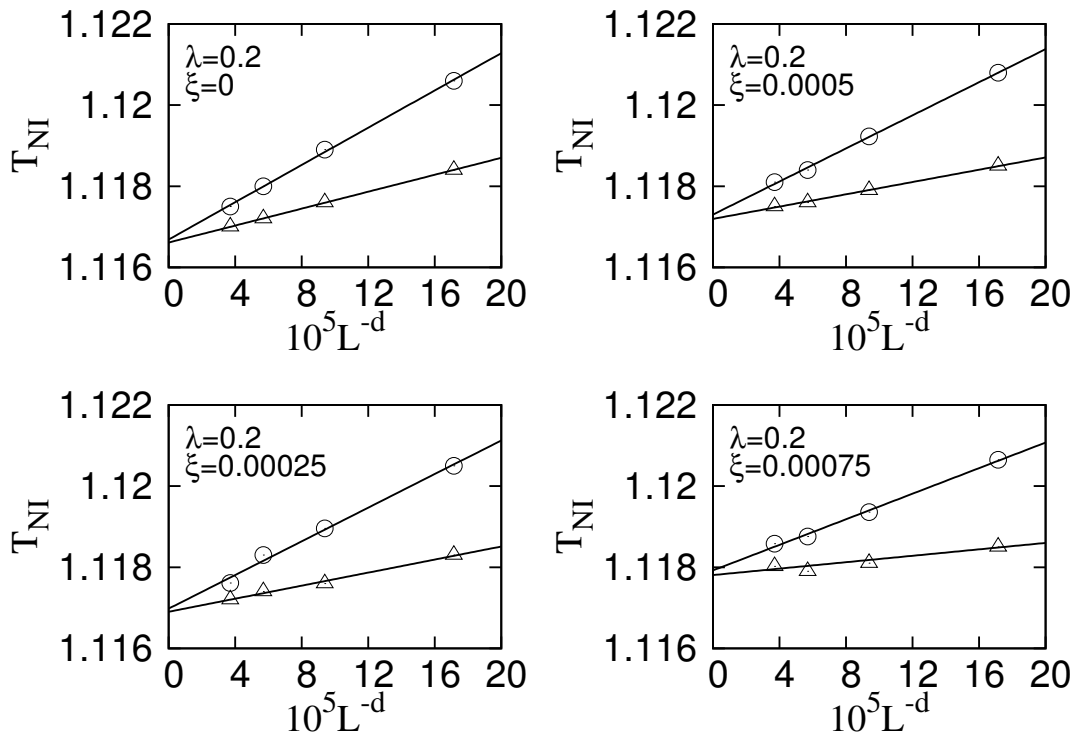


Figure 10: Finite-size scaling behaviour shown for two different measures of  $T_{NI}(L)$  for the biaxial system at four different values of  $\xi$  (the data points represented by  $\Delta$  and  $\circ$  are obtained from the peaks of  $C_v$  and  $\chi$  respectively). Extrapolations to the thermodynamic limits are denoted by solid lines.



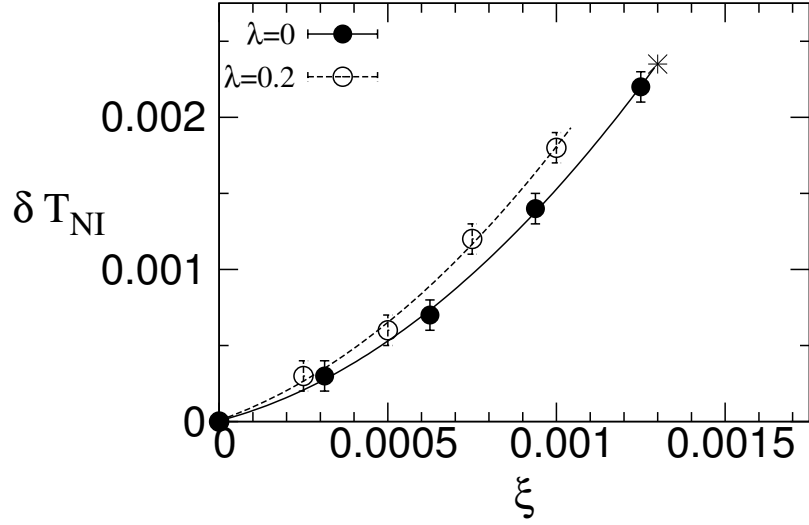


Figure 11: Increase in the NI phase transition temperature  $\delta T$  (over zero-field) vs  $\xi$  for both the uniaxial ( $\lambda = 0$ ) and biaxial ( $\lambda = 0.2$ ) models. The extrapolation of the fitted curve for  $\lambda = 0$  gives  $\delta T_{NI} = 0.00235$  for the critical parameter  $\xi_C = 0.00130$  and the symbol ( $\star$ ) represents the critical end point.

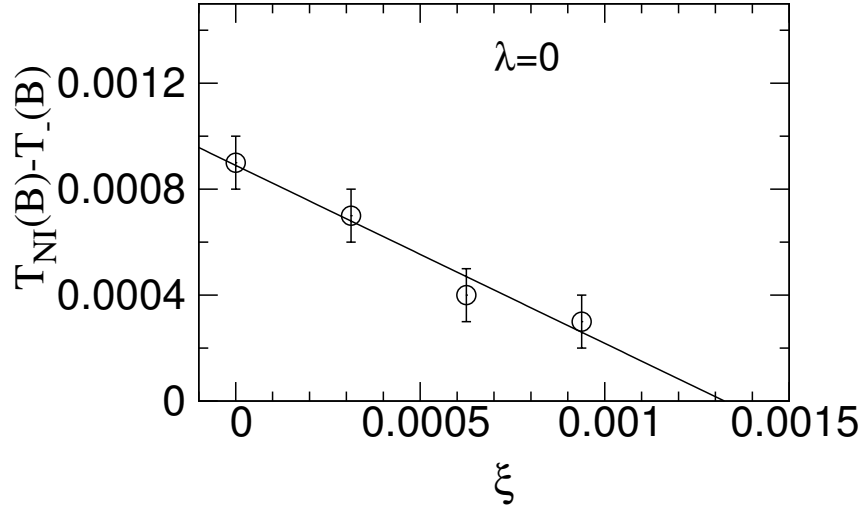


Figure 12: Plot of  $T_{NI}(B) - T_-(B)$  vs  $\xi$ . The solid line is the best linear fit. The estimated value of  $\xi_C$  is 0.00130.

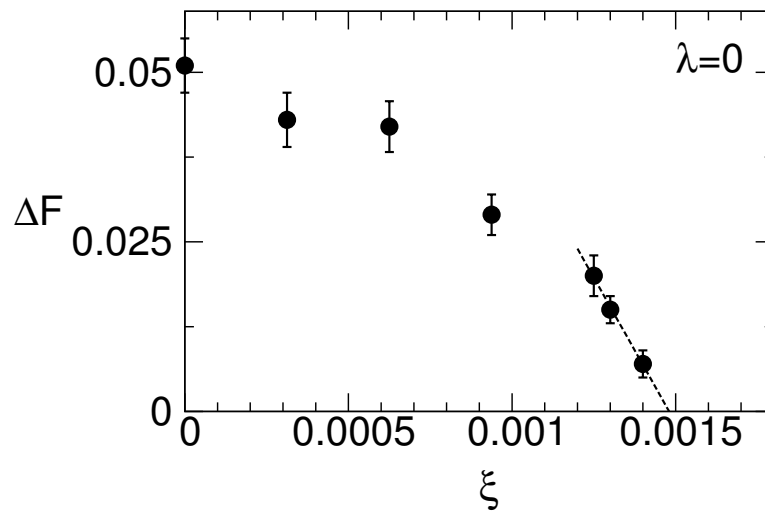


Figure 13: Free energy barrier height  $\Delta F(L)$  vs  $\xi$  for the uniaxial model and for the lattice size  $L = 30$ . A linear extrapolation of three nearest points is used to estimate  $\xi_C$  which is 0.00148.